J Mater Sci (2018) 53:8590–8603

Metals

Change in elastic properties of eutectic alloys under conditions of superplastic deformation

V. F. Korshak[1], Yu. O. Shapovalov[2,*], and P. V. Mateychenko[3]

[1] V. N. Karazin Kharkiv National University, 4 Svobody Sq., Kharkiv 61022, Ukraine
[2] B. Verkin Institute for Low Temperature Physics and Engineering of the National Academy of Sciences of Ukraine, 47 Nauky Ave., Kharkiv 61103, Ukraine
[3] Institute for Single Crystals, National Academy of Sciences of Ukraine, 60 Nauky Ave., Kharkiv 61001, Ukraine

Received: 5 September 2017
Accepted: 22 February 2018
Published online: 5 March 2018

ABSTRACT

In this study, experimental data have been obtained which reveal taking place of complex physical processes under conditions of the structural superplasticity not only in the grain boundary, as it is commonly believed, but also in the grain body. It was established for the first time that superplastic deformation of the eutectic alloys is accompanied by significant changes in their Young's moduli. It was demonstrated that under superplastic deformation the observed changes of the elastic properties of the eutectic Sn–38wt%Pb alloy under study are caused mainly by the decomposition of supersaturated solid solutions on the basis of the alloy components and the relaxation of internal stresses. It was also found that the viscous dislocation–diffusion non-conservative flow is actively developing in the eutectic alloys under conditions of superplasticity, in contrast to the existing ideas about grain boundary sliding as the main mechanism of the matter transport. The experimental results obtained are important for the deeper understanding of the physical nature of the structural superplasticity effect.

Introduction

The nature of the polycrystalline material structural state ensuring the appearance of their superplastic (SP) properties still remains one of the main unresolved problems of physics of superplasticity. One of the possible ways of solving it is the investigation of the structural and phase changes that take place under conditions of the SP flow. A large number of studies [1–5] are devoted to studying these questions. However, in most cases, changes in the microstructure of a material and, first of all, variations of a grain size are discussed.

The effect of superplasticity becomes apparent most brightly in the eutectic and eutectoid alloys [1–9], and it is referred to the structural superplasticity that reflects the traditional point of view according to which this effect is not connected with any kind of transformations in the alloys. However, in the previous studies [10–13], it was shown that the phase state of the eutectic Sn–38wt%Pb alloy which reveals SP properties does not correspond to the tin–

Address correspondence to E-mail: shapovalov@ilt.kharkov.ua

https://doi.org/10.1007/s10853-018-2163-1

lead phase diagram. It was also established that natural aging is accompanied by the change of the phase state of the alloy; however, even after a rather long aging the equilibrium is not reached [14, 15]. It is therefore natural to assume that the effect of superplasticity in the alloy results from the mutual influence of processes providing the alloy transition to the equilibrium state, which, as it is known, are stimulated by the action of the external stress and plastic deformation processes. This point is supported also by a number of results of the investigations [16] carried out at the earliest stages of the superplasticity study.

The acoustic spectroscopy methods are very sensitive to structural and phase changes in the material [17]. Nowadays, these methods are widely used for studying the properties of the materials obtained by means of the severe plastic deformation including materials that demonstrate the effect of superplasticity [18–23]. The efforts of the researchers are generally directed to studying the evolution of defective structure, the influence of internal stresses on the elastic properties after severe plastic deformation, the consideration of recovery mechanisms of the elastic modulus during annealing and natural aging of the nanostructured materials obtained by the methods of severe plastic deformation. These methods are not used for the SP flow itself.

Taking into account the above considerations the experiments have been carried out for the first time in the present investigation to study the change of Young's modulus of the eutectic Sn–38wt%Pb alloy during SP deformation (SPD) using the acoustic spectroscopy. The experiments were carried out at room temperature that allows to exclude a possible influence of quenching and high-temperature annealing on the elastic properties.

Materials and methods

The Sn–38wt%Pb alloy was prepared from pure components by melting in the laboratory furnace with a subsequent casting to a lune with the square cross section of 25 × 25 mm^2 and 5 mm depth carved in the massive copper substrate. The ingots were subjected to a preliminary uniaxial compressing between two massive plane-parallel anvils on the hydraulic press. The total deformation rate obtained was ~ 75%.

Mechanical tests were carried out under conditions of creep at an applied constant stress $\sigma = 4.5$ MPa. This stress, as it was established elsewhere [24], is optimal for the occurrence of the superplasticity effect under the selected testing conditions. Such σ value is in a good agreement with the data from Ref. [25] about the conditions of the existence of the superplasticity effect for the structural and phase state of the alloy identical to the investigated one in the present study. The initial size of the working area of the samples was 10 × 2.3 × 2 mm^3.

Acoustic measurements were carried out using a method of the two-component composite piezoelectric vibrator at a frequency of longitudinal oscillations ~ 102 and ~ 113 kHz with the amplitude of ultrasonic deformation $\varepsilon_0 \sim 10^{-7}$. The experiments were performed by the technique developed in [26].

Young's modulus was determined by the equation [17]:

$$E_S = 4\rho l_S^2 f_{0S}^2 \left(1 + k_S \frac{\pi^2 \nu^2 S}{6 l_S^2}\right), \quad (1)$$

where ρ is the density, l_s is the length, f_{0s} is the resonance frequency of the sample, ν is the Poisson's ratio, k_s is the coefficient close to 1 which exact value depends on the shape of the sample cross section with the area S. The relative error of the measurement of the Young's modulus is 0.14%.

The density of the working area of the deformed samples was determined in the following way.

Using the method of absolute hydrostatic weighing [27], the density of the entire sample was determined by the formula:

$$\rho = \frac{P_a(\rho_w - \rho_a)}{P_a - P_w} + \rho_a, \quad (2)$$

where P_a and P_w are the sample weights in the air and in the liquid, respectively, ρ_a and ρ_w are the densities of the air and the liquid at temperature and atmospheric pressure under measuring conditions. Weighing was made using the microanalytical scales with the accuracy of ± 0.00001 g. The distilled water was used as a working liquid. The data on its density are taken from [28]. The temperature during weighing was controlled with the accuracy of ± 0.25 °C.

The relative change of the sample density is equal to the relative change of its volume with the negative sign: $\Delta\rho/\rho_{in} = -\Delta V/V_{in}$, where ρ_{in} is the sample density before deformation, V_{in} is the initial volume of the sample which is defined as $V_{in} = (P_a - P_w)/$

$g\rho_w$. As it is seen from the measurements, the density of the samples heads during SPD remains almost constant. The change of the sample volume during the deformation process is determined only by the volume change of its working area. The initial volume of the working area is $V_{wa} = S_0 l_0$, where S_0 is the initial cross-sectional area and l_0 is the initial length. Thus, the change of the working area density during deformation can be calculated as follows: $\Delta\rho_{wa} = -\rho_{in}\Delta V_{wa}/S_0 l_0$ or

$$\Delta\rho_{wa} = \Delta\rho\frac{(P_a - P_w)}{g\rho_w S_0 l_0}. \quad (3)$$

The relative error of the density determination was estimated by the formula:

$$\delta\rho = \frac{\Delta mg(P_w + 2P_a)}{P_a(P_a - P_w)} + \frac{\Delta\rho_w}{\rho_w}. \quad (4)$$

The absolute error of the density value of the entire sample was $\pm$ 0.0002 g/cm^3; the absolute error of the density values of the working area did not exceed $\pm$ 0.006 g/cm^3.

Metallographic studies were carried out using the SEM and the optical microscopy techniques by means of the microscopes JSM-840 and MIM-7. The microstructure of the samples was revealed by electrolytic etching using a sequential circuit of the electrolytic bath switch on. The electrolyte solution of the following composition was taken as an etchant: 200 ml of fluoroboric acid (commercial-grade HBF_4), 20 ml of sulfuric acid (H_2SO_4, specific weight 1.84), and 780 ml of water. The required quality of revealing the structure was achieved at the bath voltage of $\sim$ 16–20 V and the current density in the sample $\sim$ 1.5 A/cm^2. The average grain size was estimated by means of the secant method.

Results

During the mechanical tests, it was found that the superplastic properties of the alloy under study depend on the duration of its aging. In particular, it was revealed that the elongation to failure δ of the samples deformed by compressing after casting increases considerably as a result of their aging for about 1.5 months. It reaches 475% at $\sigma = 4.5$ MPa. Further aging leads to the change of the flow rate of the material without a significant change in δ. The achieved experimental data are in good agreement with the results of the recently published research of peculiarities of the superplasticity effect manifestation in the investigated alloy after a high-pressure torsion [29].

Taking into account the results of the mechanical tests, the acoustic measurements were carried out on the alloy aged after preliminary compressing with aging period of $\sim$ 1.5 months. The samples were deformed to the given relative elongation, and then they were unloaded, and a part of the working area without the localized deformation regions was cut off. After the proper processing of the end faces of the obtained deformed parts, the measurements of their resonance frequency were carried out. The length of the samples prepared for the acoustic tests was 10.40 or 9.60 mm. This length corresponded to the half wave length of ultrasound in the initially compressed sample at the frequency equal to the natural frequency of the quarts oscillator. The change of the resonance frequency of the samples in comparison with the resonance frequency of the similar samples, that were preliminary subjected only to compression, has been determined. The results of the measurements are normalized to the temperature of 293 K taking into account the temperature dependence of Young's modulus of the alloy which was obtained earlier in [30].

In all cases the average value of $E = 40.04$ GPa was taken as an initial value of Young's modulus. This value was obtained from the measurements using the samples which were cut off from different parts of one and the same ingot and from different ingots.

It was established earlier [31] that the SP flow of the eutectic alloys is accompanied by the decrease in their density. Furthermore, it was found that after superplastic deformation a considerable inelastic aftereffect was observed, which is manifested by the compression of the samples and the increase in their density after unloading. In this connection, the change of the alloy density ρ during SPD process and aging in the unloaded state were determined to obtain correct data on the elastic module value.

The change of ρ depending on the exposure time t of the samples after unloading at different values of the relative elongation ε is presented in Fig. 1. The change of ρ with increasing ε is shown in Fig. 2.

The provided dependencies reflect the interval of changes of ρ observed in different samples. Points of the curves 1 and 2 are obtained by extrapolation of the experimental dependences $\rho = f(t)$ (see Fig. 1) to

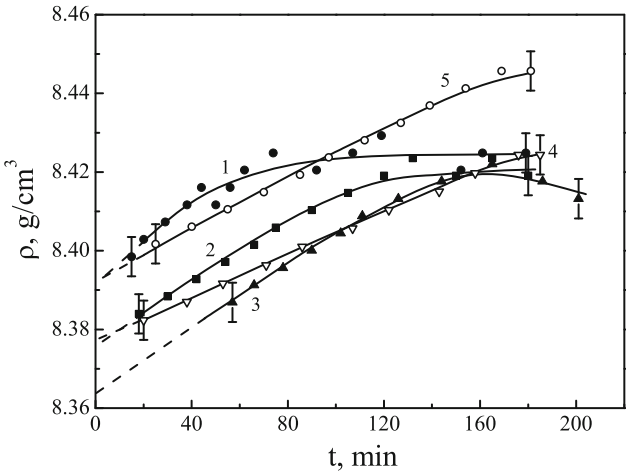

Figure 1 Density ρ of the Sn–38wt%Pb alloy as a function of the exposure time t after the deformation under conditions of superplasticity at the values of the relative elongation ε: 1–20; 2–40; 3–90; 4–140; 5–475%.

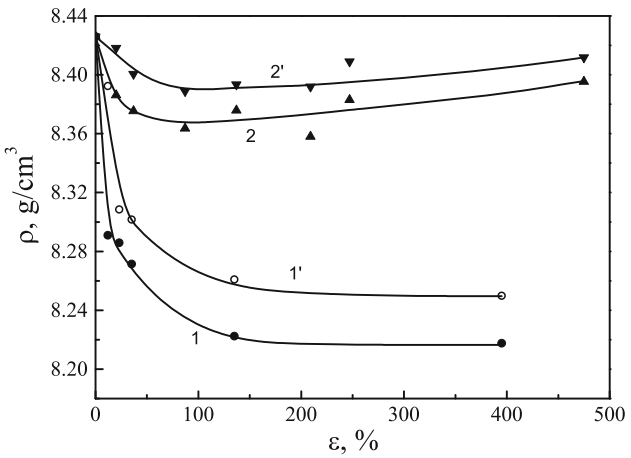

Figure 2 Density ρ of the Sn–38wt%Pb alloy as a function of the value of the relative elongation ε under optimal conditions of superplasticity (see the text).

the value $t = 0$. The curves 1′ and 2′ show the change of the density in 1 h after unloading. Approximately, such a period was required for the preparation of the samples for acoustic measurements.

As it can be seen from Fig. 2, a noticeable decrease in the density is observed with ε increasing from 0 to $\sim$ 150%, and then the value of ρ remains practically constant. The maximum relative decrease in the density reaches 2.5%.

The acoustic measurements were carried out for different values of ε in the process of the exposure of the samples in a free state during a few hours. The data on the changes of the resonant frequency and density were used to obtain the dependencies of Young's modulus of the alloy on the exposure time after SPD. To account for the length changes due to the volume change during the exposure after unloading, the initial length of the sample measured immediately prior to the acoustic measurements was multiplied by the factor $x = \sqrt[3]{V_t/V_{wa}} = \sqrt[3]{\rho_t/\rho_{wa}}$, where V_{wa} and ρ_{wa} are the volume and the density of the working area of the deformed sample before the measurement, and V_t and ρ_t are these parameters during measurement process, respectively. The change of the sample cross section during the measurements of the resonance frequency was neglected as it did not exceed an error of its experimental determination.

The relaxation curves of the elastic modulus of the alloy during the exposure of the samples which were superplastically deformed after unloading are selectively presented in Fig. 3.

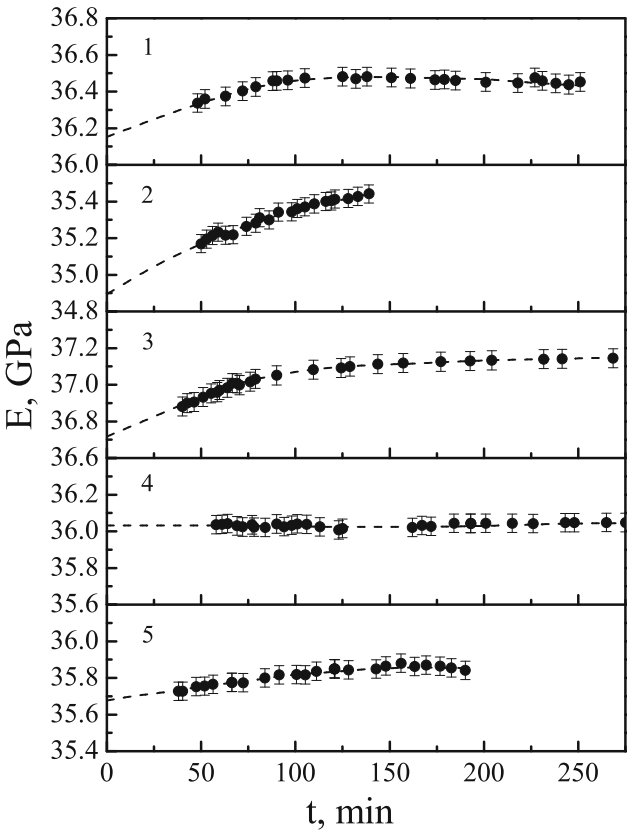

Figure 3 Change of Young's modulus E of the Sn–38wt%Pb alloy during the exposure for the time period t after unloading of a superplastically deformed samples. The relative elongation ε is: 1–21; 2–120; 3–182; 4–266; 5–350%.

The change of Young's modulus during deformation under conditions of superplasticity of the Sn–38wt%Pb alloy is shown in Fig. 4. The dependence of E on ε is obtained taking into account the results of the investigation of the modulus relaxation after unloading. The values of E were calculated using the data on the maximum change of the density during the deformation process (see curves 1, 1′ of Fig. 2). Accounting for the density changes corresponding to curves 2 and 2′ in Fig. 2 leads to the increase in E value by no more than $\sim$ 1.8%, which does not cause radical changes in the dependence of E on ε. The error shown in Fig. 4 reflects a possible dispersion of Young's modulus values which corresponds to the mean-square-root deviation σE (0.62 GPa) from the average value of Young's modulus of the alloy after the preliminary compression.

As it is shown in Fig. 4, SP flow from the very initial stages up to the relative elongations of about 150% is accompanied by a noticeable decrease in Young's modulus of the eutectic Sn–38wt%Pb alloy. At the same time, it should be noted that at the deformations of 25÷50% the change of elastic modulus has a non-monotonic character. The accumulation of the relative elongation at this stage is accompanied by an insignificant increase in E. The maximum relative decrease in E value in the experiment is about 15%. A considerable increase in Young's modulus is observed at the relative elongation of $\sim$ 200%. The further deformation leads to some decrease in E again and then Young's modulus of an alloy remains almost unchanged.

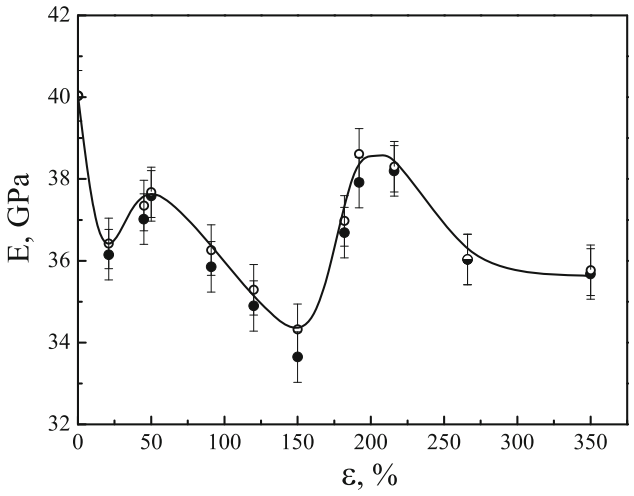

Figure 4 Dependence of Young's modulus E of the Sn–38wt%Pb alloy on the relative elongation ε under conditions of superplasticity. Open circle represents E values in 1 h after unloading. Filled circle corresponds to the values of E obtained by the extrapolation of the curve $E = f(t)$ to the time $t = 0$.

The changes of the microstructure of the alloy during SP deformation were investigated in order to establish the possible reasons of Young's modulus changes. The results of the study are presented in Fig. 5.

It was established that the average grain size of both phases in the initial state is about 3 μm. In the samples deformed up to $\sim$ 100% the elongated grains are detected in some parts of the working area, while their slight growth is registered in other parts. After deformation between 100 and 150% the appearance of the regions of significantly more fine-grained microstructure is observed (the average grain size is $\sim$ 1 μm). Many grains are extended along the direction of the external σ action (Fig. 5b, c). At the relative elongation of $\sim$ 200% the precipitation of the other phase is registered inside the grains of both phases. This process is especially brightly manifested in the α(Pb)-phase (see Fig. 5d). In the samples strongly deformed at $\varepsilon \geq 300\%$, the grains are mainly equiaxed, and their average size increases to 5.5 μm.

Metallographic studies reveal another feature of the microstructure of the superplastically deformed Sn–38wt%Pb alloy which, as far as it is known, has not been reported earlier. At large elongations, the β(Sn)-phase becomes strongly dispersed (see Fig. 5f). On the one hand, it can indicate the existence of considerable internal stresses under conditions of superplasticity and the fragmentation of β(Sn)-phase grains. On the other hand, it can be assumed that the reason for the β(Sn)-phase dispersing could also be the diffusion, activated by superplastic deformation, of lead atoms along the boundaries of subgrains and fragments, dislocation clusters and other areas of the grain structure distortions that are being formed in the process of deformation. As it was shown in [32], the diffusion of lead along the surface of tin is a thermodynamically beneficial process in the SP Sn–38wt%Pb alloy under study. A considerable part of the sample surface of this alloy is intensively covered with lead during the exposure at room temperature.

It was established, on the basis of the secant method analysis, that SPD of the alloy is accompanied by an increase in the relative fraction of β(Sn)-phase. This increase reaches 35% in the destroyed samples.

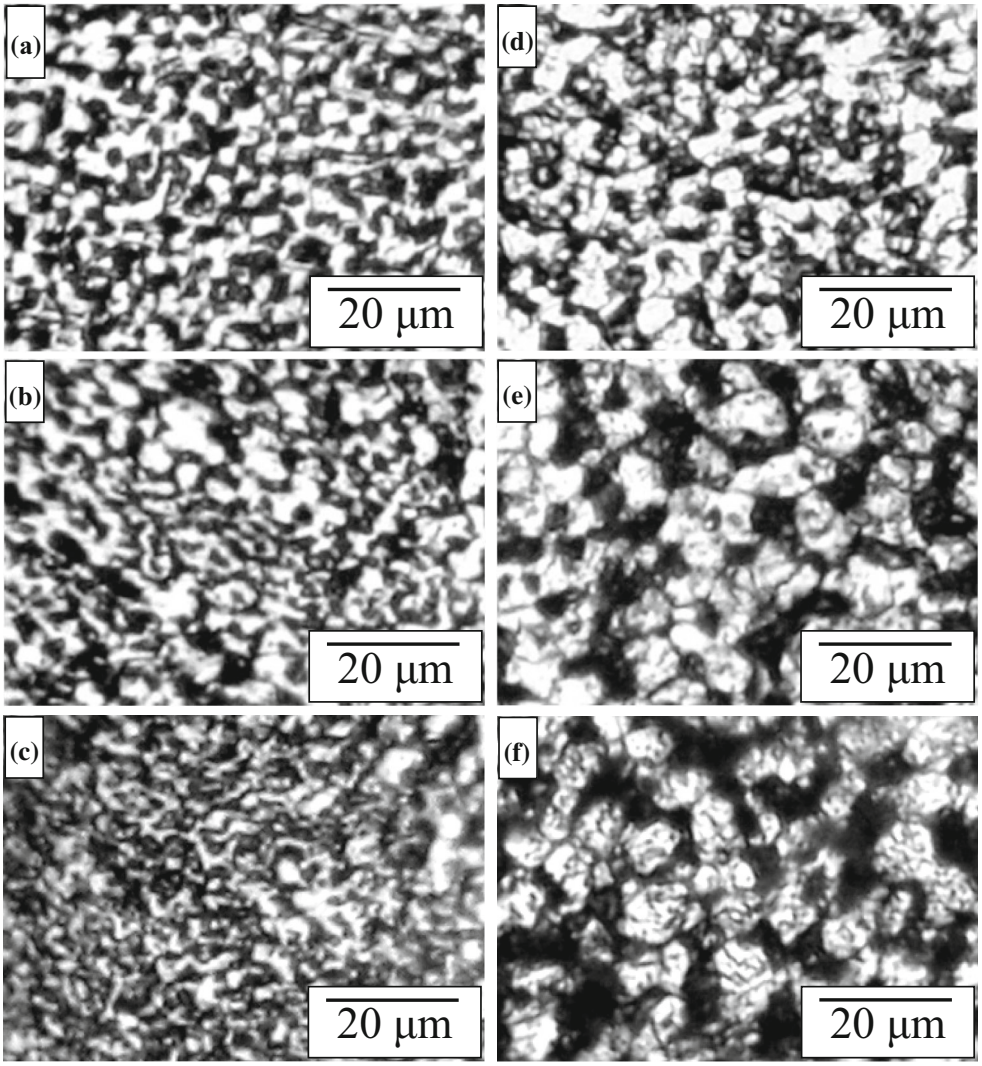

Figure 5 Optical micrographs of the surface of the Sn–38wt%Pb alloy at different stages of SP flow. The relative elongation ε is: **a** 0; **b** 120; **c** 140; **d** 200; **e**, **f** 390%. Electrolytic etching.

A decrease in the relative fraction of the α(Pb)-phase as a result of superplastic deformation is rather convincingly revealed in the analysis of the low-temperature fracture surfaces of the head and the working area of the samples (see Fig. 6).

Thus, the changes of the grain structure consisting in the change of the average grain size, the appearance of the elongated grains and areas with a fine-grained structure, the precipitation of a new phase, and the change of relative fractions of α(Pb)- and β(Sn)-phases are observed during SPD in the Sn–38wt%Pb alloy. Therefore, the experimental data obtained in the present study reveal rather a complicated nature of structural and phase transformations in the alloy, including significant changes not only in the boundary, as it is commonly believed, but also in the grain itself under conditions of structural superplasticity. These changes also do not support, in any way, the existing ideas that the main mechanism of the matter transport under conditions of superplasticity is the grain boundary sliding. In addition to the results received earlier [33] the observed peculiarities indicate the active development of a dislocation–diffusion viscous flow of the material under these conditions. It is this type of the flow which is revealed in the SEM analysis of the unprocessed surface of the samples working area after SPD (Fig. 7).

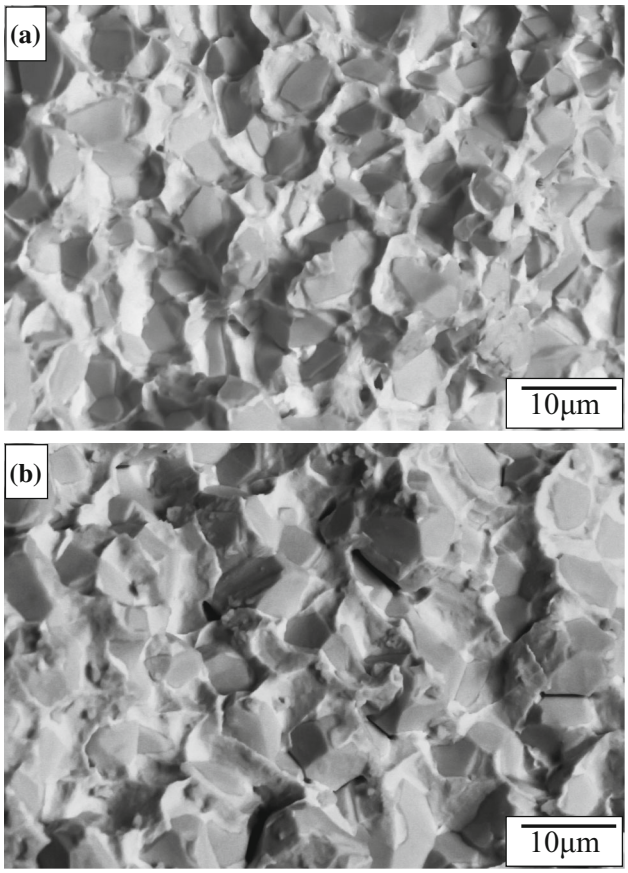

Figure 6 SEM images of low-temperature fracture surfaces of the Sn–38wt%Pb alloy aged for ~ 3 years: after a preliminary compression on the press (**a**); after superplastic deformation (**b**). Composition contrast: light areas—α(Pb)-phase; dark areas—β(Sn)-phase.

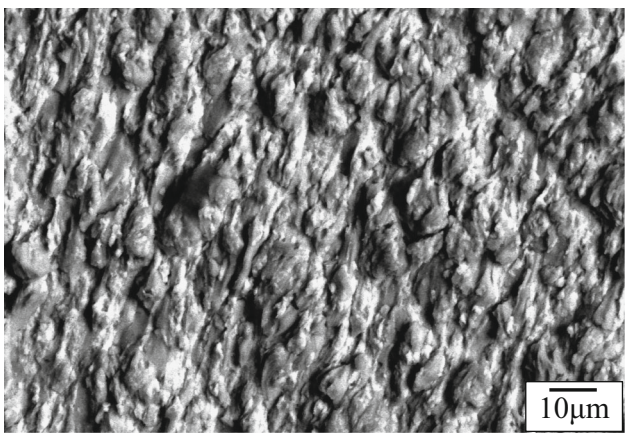

Figure 7 SEM image of the surface of the Sn–38wt%Pb alloy after superplastic deformation. Composition contrast: light and dark parts correspond to α(Pb)- and β(Sn)-phases, respectively. The direction of the strain is vertical.

Discussion

As it is known, the ability to realize SP properties is characteristic of eutectic alloys obtained under rapid crystallization conditions [1–3]. In [13] the authors found that the phase state of the investigated alloy formed by quenching of the liquid melt is characterized by a volume ratio of phases, that is by solid solutions based on tin and lead, of about 1.44:1 on average. The specified phase volume ratio in an equilibrium state at room and at eutectic temperature is 2.45:1 and 1.67:1, respectively, and the increase in Young's modulus by ~ 3% accompanies the transition from the phase state of as-cast alloy to the equilibrium phase state at room temperature [13]. Thus, the change of relative fractions of α(Pb)- and β(Sn)-phases during SP deformation, indicating the approaching of the phase state of the alloy to the equilibrium one at the room temperature, cannot be the reason of the decrease in Young's modulus registered in the experiment. An expected change of the phase state of the alloy can only make this effect less expressed.

The density change observed in the experiment (see Figure 1 and 2) that is also leads to Young's modulus change may result both from a change of the phase state of the alloy and from the appearance of porosity. According to the carried out calculations, the relative increase in the X-ray density of the Sn–38wt%Pb alloy at its transition from the equilibrium state at the eutectic temperature to the equilibrium state at the room temperature is about 0.3%. At the volume phase ratio in the alloy, registered in the experiment, the changes of the X-ray density caused by a possible change of the phase state under SPD conditions cannot differ significantly from the value above. Therefore, the change of the alloy density observed in the experiment is caused mainly by porosity.

Quite a great number of models are known to describe the dependence of the elastic characteristics of crystal materials on porosity [34, 35]. Being created for the description of different porous materials (refractory metals, ceramics, powder alloys and others), these models yield qualitatively different results at the calculation with the given value of porosity.

In some cases [36, 37] to estimate the effect of porosity on the value of Young's modulus, the conceptions of an effective Young's modulus are considered. This parameter differs from the Young's

modulus of a non-porous material because of the decrease in the effective cross section in the plane of the acting external load on the cross-sectional area of the pores in the same plane.

Let us estimate the influence of porosity on Young's modulus of the investigated alloy on the basis of the model of the elementary volume in the form of a cuboid with the initial cross section S_0. According to [36, 37], the appearance of pores with a cross section S_p in it determines the value of Young's modulus of the material equal to

$$E_{\text{eff}} = E_0(S_0 - Sp)/S_0, \tag{5}$$

where E_0 is the Young's modulus of a non-porous material.

Neglecting the change of the density due to the change of the phase composition, we determine the level of porosity P in the investigated alloy as $P = 1 - (\rho_{\text{wa}}/\rho_{\text{in}})$ or $P = |\Delta V/V_{\text{in}}|$, where ρ_{wa} is the density of the working area after SPD. If the pores are evenly distributed across the sample section, which is typical for superplastisically deformed materials [31], according to Cavalieri's principle, then $(S_0 - S_p)/S_0 = (1 - P)$.

Let us estimate, according to [38, 39], the limits of the change of Young's modulus of the alloy for the maximum pore concentration value of 2.5% using the values of the elastic modulus of a dense medium and the effective elastic modulus of the "porous phase" consisting of elementary volumes with a pore.

Averaging by Voigt [38] provides a simple connection between E_{eff} and E_0:

$$E_{\text{eff}} = E_0(1 - P). \tag{6}$$

For averaging by Reuss [39] we obtain the expression:

$$E_{\text{eff}} = \frac{E_0(C_{\text{p}} - P)}{C_{\text{p}} - P + C_{\text{p}}P}, \tag{7}$$

where C_{p} is the volume concentration of the "porous phase" which is 50% at the uniform distribution of pores, and $P = 5\%$, i.e., it is twice greater than the level of porosity in the entire sample. The calculations show that the ratio of the effective Young's modulus to the Young's modulus of a non-porous material E_{eff}/E_0 in this case ranges from 0.974 (Reuss) to 0.975 (Voigt). Therefore, the contribution of porosity to the registered change in Young's modulus does not exceed 2.5%.

This conclusion is in a good agreement with the results of the theoretical calculation of elastic constants of the porous material carried out in [40] with the use of the so-called effective medium method.

The influence of grain boundaries as a material with Young's modulus different from the elastic modulus of a crystal matrix can be attributed to another possible reasons of the decrease of Young's modulus of the alloy during SPD process.

Let us estimate the effective elastic modulus of the material E_{eff}, which is connected, according to averaging by Reuss [39], with the elastic modulus of the grain boundary E_{gb} by the following ratio: $1/E_{\text{eff}} = (1 - \alpha)/E_m + \alpha/E_{gb}$, where E_m is the elastic modulus of a crystal matrix, $\alpha = 3\Delta d/d$ is the relative volume of grain boundaries, Δd and d are the width of the boundary and the grain size, respectively. The value of an elastic modulus of a metal in an amorphous state can be taken as the Young's modulus of the boundary which, according to [41], is about 30% lower than the Young's modulus of the material in the crystalline state. The evaluations indicate that Young's modulus decrease conditioned by the appearance of the non-equilibrium boundary and by the reduce of the initial grain size to $\sim$ 1 μm with growth of the relative elongation ε to $\sim$ 150% may be not greater than 0.5%. It is necessary to point out at once that the same insignificant increase in Young's modulus can be due to the grain size growth up to $\sim$ 4 μm during a further deformation gain up to 200%. Therefore, it is obvious that one can neglect the contribution of the grain boundary as an area with a different elastic modulus, as compared to the crystal one, to the change of Young's modulus value during SPD.

The results of investigations carried out by the authors earlier in [13] agree with such a conclusion. It was established that self-annealing at room temperature of the alloy Sn–38wt%Pb during more than 1 year accompanied by the grain growth from 2 to 5 μm leads to Young's modulus increase by no more than $\sim$ 1.5%.

According to [42], the decrease in the elastic moduli of the materials, which is observed under conditions of usual plastic deformation, is a result of the action of two factors caused by the dislocation nature of the deformation process. During plastic deformation, the density of dislocations and point defects (vacancies and the dislocated atoms created by non-

conservative dislocations movement) increases. It leads to the increase in the friability of a crystal lattice, the growth of a number of places with the weakened interatomic interaction that leads to the decrease in the elastic moduli. The action of the second and the main factor is connected with the increase in a contribution of the dislocation inelasticity to the formation of the effective values of the elastic moduli. The analysis of the published data shows that at usual plastic deformation the decrease in the elastic moduli, connected with the dislocation inelasticity, is observed only at early stages of deformation of the material. In this case, plastic deformation produces the increased density of the recent dislocations without the formed dislocational atmospheres in the material. The inelasticity caused by such dislocations leads to the appearance of the modulus defect. In case of steel, for example, such effects are observed at the deformations of only 2.5–3% [42]. During the further deformation, the modulus defect usually comes to saturation and then it decreases. Therefore, if the increase of the density of the recent mobile dislocations is one of the basic reasons of Young's modulus decrease observed in the investigated alloy, then there should be a reason by which such dislocations must be intensively generated in the process of the intensive tension of the samples by 100 and more percents. The slow relaxation of the internal stresses present in the non-equilibrium alloy in the initial state can be one of such reasons. The authors have already reported the existence of significant internal elastic stresses in the initial alloy in [24].

As it is noted in [43, 44], an abrupt decrease in the elastic modulus and the formation of the additional dislocations are often observed just before the phase transformation and at its earliest stages. It can be assumed that the action of these factors is the most probable under conditions of the conducted experiment. The results of the microscopic analysis, presented in Fig. 5, the data on the change of volume fractions of α(Pb)- and β(Sn)-phases in the creep process together with the results of previous X-ray studies [32], quite convincingly show the phase transformation in the Sn–38wt%Pb alloy during SPD.

The observed Young's modulus increase with a significant relative elongation gain (see Fig. 4) can be first of all caused by the growth of a relative fraction of the β(Sn)-phase during the deformation in the alloy structure that has a greater elastic modulus if compared to the elastic modulus of the α(Pb)-phase. But, as it was already mentioned above, the transition of the alloy into the equilibrium state can lead to the elastic modulus increase only by about 3%.

A noticeable increase in Young's modulus of the alloy at $\varepsilon \sim 200\%$ can be connected with an increase in a relative fraction of the β(Sn)-phase having a much higher elastic modulus in comparison with the elastic modulus of the α(Pb)-phase with the relaxation of an initial defective alloy structure and also with the decrease in the dislocation density due to the relaxation of the internal stresses.

The texture change of the material can also provide considerable changes of Young's modulus. However, previous X-ray studies [32] show that the texture in the α(Pb)-phase is absent in samples both prepared for tests and deformed under conditions of superplasticity. There are no noticeable changes in the intensity ratio of the main lines $(200)_\alpha$, $(100)_\alpha$, $(220)_\alpha$, and $(211)_\alpha$ of the initially textured β(Sn)-phase as a result of SPD. This allows to conclude that the observed change in E value of the superplastically deformed alloy is not connected with a change in the texture of the material.

The relaxation of the initial defective structure of a material can also be a cause of the discussed increase in Young's modulus. We mean, in particular, the disappearance of an X-ray amorphous component as a result of the superplastic deformation and a vacancy supersaturation in the β(Sn)-phase [32] which are found in the alloy in an initial state. The growth of the elastic modulus can be also connected with a reduction in the dislocation density in connection with the relaxation of internal stresses. It is necessary to provide further experimental research in order to establish the role of these relaxation processes in the observed change of elastic properties of the studied alloy and, therefore, in realization of its superplastic flow.

The strain rate $\dot{\gamma}$ during the superplastic flow is usually given by a relation of the form [45–47]:

$$\dot{\gamma} = A\frac{DGb}{kT}\left(\frac{b}{d}\right)^p\left(\frac{\tau}{G}\right)^n, \tag{8}$$

where D is the appropriate diffusion coefficient, G is the shear modulus; b is the Burgers vector; k is the Boltzmann constant, T is the absolute temperature; d is the average grain size; τ is the applied shear stress; p is the exponent of the inverse grain size ($p = -\partial\ln\dot{\varepsilon}/\partial\ln d$); n is the reciprocal of strain rate sensitivity m

($n = \partial \lg \dot{\varepsilon} / \partial \lg \sigma$) [48], and A is a dimensionless constant.

Under optimal conditions for occurrence of superplasticity effect (in the region II), when grain boundary sliding is considered as the main mechanism of the mass transfer, the stress exponent n is close to 2 ($m \approx 0{,}5$), and the inverse grain size exponent p is also equal to 2 [45]. As for the constant A, as far as it is known, the available experimental data on its value strongly differ from each other and are not in good agreement with the theory. For example, for the investigated alloy at the testing temperature of 413 K in the region II, $A = 3.8 \times 10^5$ according to the experimental data, while the theory gives $A = 10$ [47]. In [46] the constant A was 1.3×10^5 for the temperature range of 336–422 K, and in [49] different values of A for the pre-eutectic and room temperatures were determined to be 8×10^6 and 59, respectively. According to some authors, parameters A and n are not independent [43].

In the investigated alloy, the average strain rate $\dot{\varepsilon}$ is 2×10^{-5} s^{-1} at $\sigma = 4.5$ MPa at room temperature. The steady-state flow is established at relative elongations of about 20% and is observed throughout almost all the deformation process of the samples. Under stresses that do not correspond to optimal conditions of superplasticity, two stages of creep are observed. At the second stage of creep, the strain rate is higher than at the initial stage.

During aging from 1 to 2 months, the average grain size in the alloy increases from $\sim$ 2.1 to $\sim$ 2.8 μm, and the strain rate at the mentioned σ decreases from 3.8×10^{-5} to 1.6×10^{-5} s^{-1}. The p parameter estimated from these data is 3.

The change of the parameter m determined from the slope of curves $\lg\sigma = f(\lg \dot{\varepsilon})$ for different stages of creep in the range of the investigated σ is presented in Fig. 8. The analysis shows that m value is changing during the deformation process of the samples at $\sigma = 4.5$ MPa. At the initial stage of creep, it is $\sim$ 0.36, and at the relative elongation of about 150% m is almost 0.5. Therefore, the parameter n in the Eq. (8) decreases from $\sim$ 2.78 to $\sim$ 2.0.

Let us estimate constant A using the obtained experimental data and the known relations between the shear stress and the strain rate (τ and $\dot{\gamma}$) and the normal stress and the strain rate (σ and $\dot{\varepsilon}$) [50], and also the relations between the shear modulus and Young's modulus ($G = E/2(1 + \mu)$, where μ is the Poisson ratio). A appears to be equal to 3.4×10^{10} at

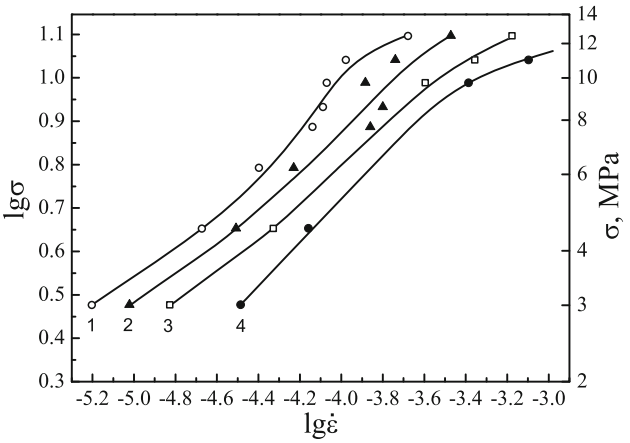

Figure 8 Dependence of lgσ on lg for Sn–38wt%Pb alloy at different relative elongations ε: 1–22, 2–50, 3–100, 4–146%. T = 293 K. The values on the abscissa axis refer to curve 1. The difference in actual values of the abscissa axis for curves 1–2, 2–3, and 3–4 is 0.2.

the initial stage of creep and 2.6×10^6 at the relative elongation of about 150%. The estimated grain size d is $\sim$ 2.5 μm in the former case, and $\sim$ 1 μm in the latter case (see Fig. 5a, c). According to [47], Burgers vector b in the investigated alloy is 3.2×10^{10} m. The grain boundary diffusion coefficient D_{gb} determined in [51] for Sn–38wt%Pb alloy at room temperature is $\approx 10^{-14}$ m/s^2.

Thus, according to the existing conceptions [47, 52], the deformation under conditions of superplasticity in the investigated alloy at the initial stages is controlled by the dislocations glide ($n = 3$) and the grain boundary diffusion ($p = 3$). This conclusion is in good agreement with the results of the study of microstructural changes in the alloy under conditions of superplasticity which was carried out by the authors earlier in [12, 33]. As it is shown in these papers, SPD in the alloy is starting from the appearance of the localized deformation bands similar to the Lüders band with their subsequent spreading all over the section of the sample. When the elongation is about 150%, the flow of the material gains the rheological features of the superplasticity region II ($n = 2$). However, at the same time, we do not observe the development of the grain boundary sliding in the investigated alloy. At this stage, as it was already noted, the viscous dislocation–diffusion non-conservative flow of the material is actively implemented, the hydrodynamic deformation mode becomes apparent [12, 33]. It should be noted that we also observed a similar nature of microstructural

changes under conditions of superplasticity in the eutectic alloy Bi–43wt%Sn [53].

According to the deformation mechanism map for the investigated alloy constructed in [54], mechanical tests in this study were carried out under conditions corresponding to the transition area of the rate dependence of phenomenological parameters of the superplastically deformed materials from the region I to the region II. According to [45] the constant A in the region I for the investigated alloy is equal to 1.5×10^{14}, and in the region II, as it was already noted, $A = 3.8 \times 10^5$ in the case of the deformation at the pre-eutectic temperature. Such a change of A is qualitatively similar to its changes observed in the present experiment during the samples elongation in spite of the fact that quantitative values are considerably different. However, this can be due to the difference in the deformation temperature. From the physical point of view, this can reveal a certain analogy in the change of the deformation mechanisms realized in both cases. This, in turn, can support the ideas presented in [12, 33, 53] concerning the important role of the dislocation glide in the creation of the structural-phase state that ensures the realization of the superplasticity effect in the investigated eutectic alloys.

Finally, one more feature of the plastic behavior of the studied Sn–38wt%Pb alloy under the chosen test conditions should be noted. As it can be seen in Fig. 8 at the initial stages of the deformation, the parameter m has the maximum value at stresses higher than 4.5 MPa. In this range, another maximum is also observed on the curve $\delta = f(\sigma)$. However, the elongations reached are significantly lower and δ is about 200%. The decrease in the parameter m as the deformation develops at elevated stresses (see Fig. 8) indicates the structure changes in the alloy that are negatively effecting its superplastic properties. This may be due to the unconformity of the kinetic features of the processes caused by the plastic deformation and the phase transition that occurs meanwhile. However, these questions were not the subject of this research.

The results received in the present study, together with results published earlier in [10–15, 24, 30–33, 53], demonstrate the variety of physical processes which occur in the eutectic alloys under conditions of SP deformation. They confirm the opinion of the authors that the effect of superplasticity in the eutectic alloys is the result of the mutual influence of the processes of the plastic flow and the phase transitions in initially metastable materials. The obtained results also supplement the available databank on rheological parameters of the superplastic deformation of polycrystalline metallic materials.

Conclusions

1. For the first time the Young's modulus changes of the eutectic Sn–38wt%Pb alloy under conditions of superplastic deformation have been studied. The acoustic spectroscopy method was applied. It has been shown that these changes have a complex non-monotonic character. SP flow at the initial stages is accompanied by a considerable decrease in Young's modulus of the alloy. The maximum decrease in the modulus value is observed at the elongation of about 150% and is of $\sim$ 15%. At later stages of the deformation, a significant increase in the elastic modulus and its subsequent decrease are registered.
2. Superplastic deformation of the eutectic Sn–38wt%Pb alloy is accompanied by the changes of its structural and phase state consisting in the change of an average grain size, the appearance of the elongated grains, the appearance of the areas with a more fine-grained structure compared to the initial one, a new phase precipitation, a change of relative fractions of α(Pb)- and β(Sn)-phases and the dispersion of the β(Sn)-phase. These data demonstrate the variety of structural and phase transformations which are realized under conditions of superplasticity in the alloys of the studied type unlike the data on the preservation of equiaxed grains and the increase in the linear grain size which are traditionally reported in the literature.
3. The observed change of Young's modulus of the eutectic Sn–38wt%Pb alloy during the SP flow can be caused by the realization of the initial stage of the decomposition of the supersaturated solid solutions stimulated by the plastic deformation, by a change of the relative fractions of phases in the alloy structure, by the relaxation of internal stresses, and by the change of the dislocation density and the concentration of vacancies, connected with it, and by the change of the alloy density as well.

4. The realization of structural and phase changes caused by the non-equilibrium initial phase state provides the active development of the viscous dislocation–diffusion non-conservative flow in the eutectic alloys under the superplastic deformation. This kind of the matter transport is dominant in contrast to the existing traditional ideas about the grain boundary sliding as the main deformation mechanism under superplasticity conditions.
5. The obtained experimental results are in good agreement and essentially complete the authors' views on the structural superplasticity as the effect arising as a result of the mutual influence of the processes of the plastic deformation and the phase transformation in the initially non-equilibrium systems.

Acknowledgements

The authors are grateful to P.P. Pal-Val, Dr. Sci., the Head of the Department of B. Verkin Institute for Low Temperature Physics and Engineering of the National Academy of Sciences of Ukraine, for the assistance in making acoustic experiments and useful consultations. This research did not receive any specific grant from funding agencies in the public, commercial, or not-for-profit sectors.

Compliance with ethical standards

Conflict of interest The authors declare that they have no conflict of interests.

References

[1] Kaibyshev OA (1992) Superplasticity of alloys, intermetallides and ceramics. Springer, Berlin
[2] Nieh TG, Wadsworth J, Sherby OD (1997) Superplasticity in metals and ceramics. Cambridge University Press, Cambridge
[3] Gilliano G (ed) (2011) Superplastic forming of advanced metallic materials: methods and application. Woodhead Publishing Limited, Cambridge
[4] Langdon TG (2009) Seventy-five years of superplasticity: historic developments and new opportunities. J Mater Sci 44:5998–6010. https://doi.org/10.1007/s10853-009-3780-5
[5] Langdon TG (2013) Twenty-five years of ultrafine-grained materials: achieving exceptional properties through grain refinement. Acta Mater 61:7035–7059. https://doi.org/10.1016/j.actamat.2013.08.018
[6] Kawasaki M, Foissey J, Langdon TG (2013) Development of hardness homogeneity and superplastic behavior in an aluminum–copper eutectic alloy processed by high-pressure torsion. Mater Sci Eng A 561:118–125. https://doi.org/10.1016/j.msea.2012.10.096
[7] Ahmed MMI, Langdon TG (1983) Ductility of the superplastic Pb–Sn eutectic at room temperature. J Mater Sci Lett 2:59–62
[8] Ahmed MMI, Langdon TG (1983) The effect of grain size on ductility in the superplastic Pb–Sn eutectic. J Mater Sci Lett 2:337–340
[9] Cho TS, Lee HJ, Ahn B, Kawasaki M, Langdon TG (2014) Microstructural evolution and mechanical properties in a Zn–Al eutectoid alloy processed by high-pressure torsion. Acta Mater 72:67–79. https://doi.org/10.1016/j.actamat.2014.03.026
[10] Korshak VF, Arzhavitin VM, Rozumnii OS (1999) Young's modulus change of the Pb–62% Sn superplastic alloy upon deformation. Vestn Khark Gos Univ Ser Phys 3:76–79 **(in Russian)**
[11] Korshak VF, Arzhavitin VM, Samsonik AL, Mateichenko PV (2005) Metastability and structure-phase transformations in a tin–lead superplastic eutectic alloy. Izv Akad Nauk Ser Fiz 69:1543–1547
[12] Korshak VF, Kryshtal' AP, Mateychenko PV, Sirenko AF (2007) Strain-induced structural and phase transitions in superplastic eutectic. Bull Russ Acad Sci Phys 71:1680–1684. https://doi.org/10.3103/S1062873807120064
[13] Korshak VF, Shapovalov YuA, Pal'-Val' PP, Mateichenko PV (2011) Changes in the structural phase state and elastic and inelastic properties of superplastic eutectic Sn–38% wt Pb alloy during the aging process. Bull Russ Acad Sci Phys 75:1345–1351. https://doi.org/10.3103/S1062873811100200
[14] Korshak VF, Shapovalov YuA, Mateychenko PV, Danilina IA (2008) Change of a structure-phase state and superplastic properties of tin-lead eutectics during aging process. Metallofiz Noveishie Tekhnol 30:385–396 **(in Russian)**
[15] Korshak VF, Shapovalov YuA (2009) Some aspects of superplastic flow of eutectic alloys connected with metastability. Phys Met Metallogr 107:394–399. https://doi.org/10.1134/S0031918X09040103
[16] Presnyakov AA (1976) Superplasticity of metals and alloys. British Library Lending Division, Boston
[17] Nikanorov SP, Kardashov BK (1985) Elasticity and dislocation anelasticity of crystals. Nauka, Moscow **(in Russian)**

[18] Burenkov YuA, Nikanorov SP, Smirnov BI, Kopylov VI (2003) Recovery of Young's modulus upon annealing of nanostructured niobium produced through severe plastic deformation. Phys Solid State 45:2119–2123. https://doi.org/10.1134/1.1626747

[19] Kardashev BK, Plaksin OA, Stepanov VA, Chernov VM (2004) Effect of proton and laser irradiation on the elastic and inelastic properties of a V–Ti–Cr alloy. Phys Solid State 46:1449–1455. https://doi.org/10.1134/1.1788777

[20] Betekhtin VI, Kadomtsev AG, Kardashev BK (2006) Elasticity and anelasticity of microcrystalline aluminum samples having various deformation and thermal histories. Phys Solid State 48:1506–1512. https://doi.org/10.1134/S1063783406080142

[21] Betekhtin VI, Sklenicka V, Saxl I, Kardashev BK, Kadomtsev AG, Narykova MV (2010) Influence of the number of passes under equal-channel angular pressing on the elastic-plastic properties, durability, and defect structure of the Al + 0.2 wt% Sc alloy. Phys Solid State 52:1629–1636. https://doi.org/10.1134/s1063783410080111

[22] Ahmadeev NH, Kovelev NP, Mulyukov RR, YaM Soifer, Valiev RZ (1993) The effect of heat treatment on the elastic and dissipative properties of copper with the submicrocrystalline structure. Acta Metall Mater 41:1041–1046. https://doi.org/10.1016/0956-7151(93)90153-J

[23] Lebedev AB, Pulnev SA, Kopylov VI, Burenkov YuA, Vetrov VV, Vylegzhanin OV (1996) Thermal stability of submicrocrystalline copper and Cu: ZrO_2 composite. Scr Mater 35:1077–1081. https://doi.org/10.1016/1359-6462(96)00261-8

[24] Korshak VF, Shapovalov YuA, Vaselenko NN (2015) Structural and phase relaxation in superplastic eutectic alloy Sn–38% wt. Pb. Metallofiz Noveishie Tekhnol 37:1633–1642 **(in Russian)**

[25] Soliman MS (1994) Superplastic characteristics of the Pb-62%Sn eutectic alloy at room temperature. Scr Metall Mater 31:439–444. https://doi.org/10.1016/0956-716X(94)90015-9

[26] Natsik VD, Pal-Val PP, Smirnov SN (1998) Theory of a compound piezoelectric vibrator. Akust Zhurnal 44:640–647 **(in Russian)**

[27] Bowman HA, Schoonover RM (1967) Procedure for high precision density determinations by hydrostatic weighing. J Res Natl Bur Stand C 71:179–198. https://doi.org/10.6028/jres.071C.017

[28] Haynes WM (ed) (2014) CRC handbook of chemistry and physics, 95th edn. CRC Press, Boca Raton

[29] Zhang NX, Chinh NQ, Kawasaki M, Huang Y, Langdon TG (2016) Self-annealing in a two-phase Pb–Sn alloy after processing by high-pressure torsion. Mater Sci Eng A 666:350–359. https://doi.org/10.1016/j.msea.2016.04.058

[30] Pal-Val LN, Pal-Val PP, Korshak VF, Mateychenko PV (2008) The effect of aging on the elastic and anelastic properties of a eutectic alloy Sn-38 wt%Pb. Condens Matter Interfaces 1:50–53 **(in Russian)**

[31] Korshak VF, Kuznetsova RI, Zu CT (1990) Aftereffect in superplactically deformed alloy Pb-62%Sn. Fiz Met Metalloved 5:184–187 **(in Russian)**

[32] Korshak VF, Shapovalov YuA, Samsonik AL, Mateichenko PV (2012) X-ray diffraction study of structural and phase states of a superplastic Sn-38 wt% Pb alloy and their variations under the effect of external mechanical stresses and aging. Phys Met Metallogr 113:190–199. https://doi.org/10.1134/S0031918X1202007X

[33] Korshak VF, Kryshtal' AP, Shapovalov YuA, Samsonik AL (2010) Hydrodynamic flow of the eutectic under the conditions of superplasticity. Phys Met Metallogr 110:385–393. https://doi.org/10.1134/S0031918X10100091

[34] Broutman LJ (ed) (1974) Composite materials, vol 4. Academic Press, Cambridge

[35] Yoshimura HN, Molisani AL, Narita NE, Cesar PF, Goldenstein H (2007) Porosity dependence of elastic constants in aluminum nitride ceramics. Mater Res 10:127–133. https://doi.org/10.1590/S1516-14392007000200006

[36] IgS Konovalenko, Smolin AYu, Korostelev SYu, Psakh'e SG (2009) Dependence of the macroscopic elastic properties of porous media on the parameters of a stochastic spatial pore distribution. Tech Phys 54:758–761. https://doi.org/10.1134/S1063784209050272

[37] Polyakov VV, Egorov AV, Turetskii VA (2004) Elastic moduli of porous pseudoalloy. News Altai State Univ 31:119–121 **(in Russian)**

[38] Voight W (1928) Lehrbuch der Kristallphysik. Berlin, Teubner. https://doi.org/10.1007/978-3-663-15884-4 **(in German)**

[39] Reuss A (1929) Berechnung der Fliebgrenze von Misehkristallen auf Grund der Plastizitätsbedingung für Einkrestalle. Z Angew Math Mech 9:49–58. https://doi.org/10.1002/zamm.19290090104 **(in German)**

[40] Apalkov VM, Boiko YuI, Slezov VV, Hoffmann MJ (2001) The elastic constants of porous medium. Sci Sinter 33:21–29

[41] Valiev RZ, Alexandrov IV (2007) Bulk nanostructured metallic materials. IKTs "Akademkniga", Moscow

[42] Golovin SA, Pushkar A, Levin DM (1987) Elastic and damping properties of structural metallic materials. Metallurgiya, Moscow (**in Russian**)

[43] Poirier JP (1985) Creep of crystals. High temperature deformation processes in metals, ceramics and minerals. Cambridge University Press, Cambridge

[44] Poirier JP (1982) On transformation plasticity. J Geophys Res 87:6791–6797. https://doi.org/10.1029/JB087iB08p06791

[45] Kawasaki M, Langdon TG (2015) Developing superplasticity in ultrafine-grained metals. Acta Phys Pol A 128:470–478. https://doi.org/10.12693/APhysPolA.128.470

[46] Langdon TG, Mohamed FA (1977) The activation energies for superplasticity. Scr Metall 11:575–579. https://doi.org/10.1016/0036-9748(77)90112-0

[47] Kawasaki M, Lee S, Langdon TG (2009) Constructing a deformation mechanism map for a superplastic Pb–Sn alloy processed by equal-channel angular pressing. Scr Mater 61:963–966. https://doi.org/10.1016/j.scriptamat.2009.08.001

[48] Mohamed FA, Langdon TG (1975) Creep behaviour in the superplastic Pb-62% Sn eutectic. Philos Mag 32:697–709. https://doi.org/10.1080/14786437508221614

[49] Pink E, Kutschej R, Stüwe HP (1981) Evidence for lattice-diffusion controlled superplasticity in a Sn–Pb–eutectic. Scr Metall 15:185–189. https://doi.org/10.1016/0036-9748(81)90326-4

[50] Ashby MF (1983) Mechanisms of deformation and fracture. Adv Appl Mech 23:117–177. https://doi.org/10.1016/S0065-2156(08)70243-6

[51] Gupta D, Vieregge K, Gust W (1999) Interface diffusion in eutectic Pb–Sn solder. Acta Mater 47:5–12. https://doi.org/10.1016/S1359-6454(98)00348-6

[52] Langdon TG (2006) Grain boundary sliding revisited: developments in sliding over four decades. J Mater Sci 41:597–609. https://doi.org/10.1007/s10853-006-6476-0

[53] Korshak VF, Shapovalov YuA, Prymak O, Kryshtal AP, Vasilenko RL (2015) Structural changes in Bi-43 wt% Sn eutectic alloy under superplastic deformation. Phys Met Metallogr 116:829–837. https://doi.org/10.1134/S0031918X15060034

[54] Pink E, Márquez A, Grinberg A (1981) A note on rate sensitivities of flow stresses of eutectic and eutectoid alloys. Scr Metall 15:191–194. https://doi.org/10.1016/0036-9748(81)90327-6